Resonance photoemission for f-electron systems

O. Gunnarsson and T. C. Li

Max-Planck-Institut für Festkörperforschung, D-7000 Stuttgart 80, West Germany

We develop a theory for resonance photoemission and apply it to Ce compounds and UO_2 described in a modified Anderson impurity model. For Ce (UO_2) the model takes into account decay processes involving two $4f$ ($5f$) electrons, one $4f$ ($5f$) electron, and a core electron. Starting from the quadratic response formalism, we derive general formulas for the photoemission spectrum as a function of photon energy. The $1/N_f$ expansion is then used to obtain explicit results for the Anderson model. All terms of order $(1/N_f)^0$ and some terms of order $(1/N_f)^1$ are included. The theory is used to explain the different photon-energy dependence for the two peaks in the Ce $4f$ valence and the UO_2 $4f$ core spectra. We find that interference between different intermediate configurations plays a crucial role.

I. INTRODUCTION

The valence photoemission spectra of Ce compounds have greatly contributed to our understanding of these systems in general and the role of the f electrons in particular.[1,2] The separation of the $4f$ and conduction-band contributions to the valence spectrum is, however, by no means trivial. One method uses the different photon-energy dependencies of the $4f$ and conduction-band emission in the range 20–80 eV.[3,4] A second method uses the fact that the $4f$ cross section shows a resonance for the photon energy $\hbar\omega \sim 122$ eV.[5,6] The second method has been widely used, in particular for the frequently studied compounds with late transition elements,[1,2] for which the d-band emission tends to dominate the spectrum for photon energies in the range 20–80 eV. Recently, resonance photoemission has also been used for U compounds.[7,8] In particular the $4f$ core spectrum of UO_2 has been studied.[7]

For Ce the resonance in the cross section occurs due to the transition $4d \rightarrow 4f$ which is followed by an Auger decay. The $4f$ emission results from the "resonance" process

$$[\text{core}]4d^{10}V^{4-n}4f^n \rightarrow [\text{core}]4d^9V^{4-n}4f^{n+1}$$

$$\rightarrow [\text{core}]4d^{10}V^{4-n}4f^{n-1}\epsilon l , \qquad (1.1)$$

where V represents conduction states and ϵl the continuum states. The final state in Eq. (1.1) is the same as for the "direct" process

$$[\text{core}]4d^{10}V^{4-n}4f^n \rightarrow [\text{core}]4d^{10}V^{4-n}4f^{n-1}\epsilon l , \qquad (1.2)$$

and the *amplitudes* of the two processes have to be added. The total cross section shows a resonance at $\hbar\omega \sim 122$ eV, since this is close to the energy required for the $4d \rightarrow 4f$ transition in Eq. (1.1). There are several other processes competing with the second transition in Eq. (1.1), leading to $5p$, $5s$, $4d$, and conduction-band emission. For UO_2, the resonance in the $4f$ core spectrum due to a $3d \rightarrow 5f$ transition has been studied.[7]

Valence photoemission spectra of Ce compounds typically show two structures, one at -2 eV and one close to the Fermi energy $\epsilon_F = 0$ eV.[9,10] The constant-initial-state (CIS) spectra for these two features show somewhat different photon-energy dependencies,[10] suggesting that they may have different characters. Later work has provided much evidence that both structures have a substantial amount of $4f$ character,[3,11] but it has remained a puzzle why the two structures have different photon-energy dependencies.

After resonance photoemission had been observed for Ni,[12] there were several theoretical studies of resonance photoemission focusing on the mechanism for the resonance and its application to, in particular, the $3d$ compounds.[13,14] In spite of the great practical importance of resonance photoemission for the study of Ce compounds, there has been little theoretical work for these systems. Zangwill and Soven[15] used the density-functional formalism in a study of the photon-energy dependence of the total and partial cross sections. Sakuma et al.[16] studied resonance photoemission for a generalized Anderson model[17] in the limit of an infinite $4f$-$4f$ Coulomb interaction U. They calculated the CIS spectra of the two structures in the Ce $4f$ spectrum and found that these can be different. We have found, however, that for the $U = \infty$ limit, different photon-energy dependencies can be obtained only on the energy scale of the so-called Kondo temperature T_K, and that it is important to take into account that U is finite.[18]

Most theoretical work on photoemission has used the so-called sudden approximation, which neglects the interaction between the emitted electron and the $(N-1)$-electron system left behind.[19] One then only needs to study the $(N-1)$-electron system. In resonance photoemission we include the Auger transition

$$4d^9 4f^{n+1} \leftrightarrow 4d^{10}4f^{n-1}\epsilon l . \qquad (1.3)$$

Since this process can go in either direction, it implies an interaction between the emitted electron ϵl and the $(N-1)$-electron system. This leads to transitions of the

type

$$[4d^{10}4f^{n-1}]^m \epsilon l \rightarrow [4d^9 4f^{n+1}]^{m'} \rightarrow [4d^{10}4f^{n-1}]^{m''} \epsilon' l \ ,$$

$$(1.4)$$

where the index m refers to different states. In the formalism below we only include interaction with the emitted electron of this type. We can then use a projection-operator formalism developed for the description of incomplete relaxation in Auger electron spectroscopy.[20] It is possible to express the spectrum in terms of

$$P_f(\varepsilon,\omega) = \langle \tilde{E}_0(\omega) \mid \delta(\varepsilon - E_0(N) + H) \mid \tilde{E}_0(\omega) \rangle \ , \qquad (1.5)$$

where $\mid \tilde{E}_0(\omega) \rangle$ does not contain the emitted electron explicitly. The state $\mid \tilde{E}_0(\omega) \rangle$ is ω dependent due to the resonance effect, and the resonance is broadened and distorted due to the interaction with the emitted electron. In (nonresonance) photoemission this state is replaced by $\psi_\nu \mid E_0(N) \rangle$, where ψ_ν annihilates an f electron and $E_0 \mid (N) \rangle$ is the ground state. Once the state $\mid \tilde{E}_0(N) \rangle$ has been calculated, the problem is reduced to a calculation equivalent to the (nonresonance) photoemission calculation using the sudden approximation. The latter calculation can be performed by one of the methods developed earlier.[21-23]

As a model for the Ce compounds, we have used a generalized Anderson model.[17] This model includes the degenerate $4f$ level, the conduction states, and the hopping between these states. Furthermore the Coulomb interaction U between the $4f$ electrons is included. This model has been demonstrated to give a good description of Ce compounds.[2,23] The model is generalized by including the appropriate Auger decay terms and the Coulomb interaction between the core levels and the $4f$ level.

The same model is also applied to UO_2. While multiplet effects are important for some properties of Ce, many properties are dominated by the f^0 and f^1 configurations, which have no multiplet effects. For U, on the other hand, the important configurations are $5f^2$ and $5f^3$ and we expect multiplet effects to be important, in general. For UO_2, however, the hybridization

$(N_f \Delta \sim 11$ eV) is larger than the multiplet splitting and comparable to the energy separation between the different configurations. We therefore expect that the different multiplets will be mixed into the ground state (see also Appendix A in Ref. 21). In a first approximation we can then neglect the multiplet splitting. Some aspects of this work were presented in Ref. 18.

II. MODEL

We use the Anderson impurity model in the form

$$H_0 = \sum_{\nu=1}^{N_f} \left[\int d\varepsilon \, \varepsilon \psi_{\varepsilon\nu}^\dagger \psi_{\varepsilon\nu} + \varepsilon_f \psi_\nu^\dagger \psi_\nu \right.$$
$$\left. + \int d\varepsilon [V(\varepsilon) \psi_\nu^\dagger \psi_{\varepsilon\nu} + \text{H.c.}] \right]$$
$$+ U \sum_{\nu < \mu} n_\nu n_\mu \ , \qquad (2.1)$$

where the first term describes the conduction states, the second the f level, the third the hopping between these two types of states, and the fourth the Coulomb interaction. Here ε_f is the f-level energy, $V(\varepsilon)$ is a hybridization matrix element, and U is the f-electron Coulomb interaction. The f level has the degeneracy N_f and the index ν describes the spin and orbital indices. The conduction states have been transformed to the same representation ν.[21] Equation (2.1) only includes the states which couple to the f state after this transformation. The other states do not influence the calculations and are therefore not included. Equation (2.1) is an impurity model, i.e., only the f level on one Ce atom is treated explicitly. This model has been used frequently for the description of Ce compounds, as reviewed in Refs. 2 and 23, for instance, in the work of Gunnarsson and Schönhammer,[21-23] Wuilloud $et\ al.,$[24] Delley and Beck,[25] Sakai $et\ al.,$[26] and Bickers $et\ al.$[27] Following Herbst $et\ al.,$[28] it is assumed that the f-f Coulomb interaction U is the essential one, and that other interactions can be included implicitly as a renormalization of U.[2,23] The model has been discussed extensively in Ref. 23.

We further include a term describing the $4d$ level and its interaction with the $4f$ level

$$H_{4d} = \varepsilon_{4d} \sum_\nu \psi_{d\nu}^\dagger \psi_{d\nu} + \left[N_f - \sum_\nu \psi_{d\nu}^\dagger \psi_{d\nu} \right] \left[\sum_n (\varepsilon_M^{(n)} - n U_{fc}) P_n + \left[\int d\varepsilon (C_M - 1) V(\varepsilon) \psi_\nu^\dagger \psi_{\varepsilon\nu} + \text{H.c.} \right] \right] \ . \qquad (2.2)$$

The $4d$ level, with energy ε_{4d}, is, for simplicity, assumed to have the degeneracy N_f. In view of the simplicity of the model, e.g., the neglect of multiplet effects, the extra effort in taking into account the different degeneracies of the $4d$ and $4f$ levels does not seem justified. The operator P_n projects out states with n $4f$ electrons. The second term in (2.2) is zero if the $4d$ level is filled. This term describes how the $4f$ configurations are shifted in the presence of a $4d$ core hole. In core-level x-ray pho-

toemission spectroscopy (XPS) the f configurations are assumed to be lowered by U_{fc}, due to the core hole attraction.[29,21] The dipole transition $4d \rightarrow 4f$, however, gives most of the weight for multiplets which are shifted upwards in energy.[30] Since we neglect multiplet effects, Eqs. (2.1) and (2.2) only allow one energy for each configuration. We therefore introduce $\epsilon_M^{(n)} > U_{fc}$ to describe the upward shift of the most important multiplets. Due to this upward shift of the $4f$ level, one may expect

the $4f$ orbital to expand. This increases the coupling to the conduction states, as is described by the last part of the second term. In the presence of a $4d$ core hole, the hopping matrix element is thus assumed to be $C_M V(\varepsilon)$. We also include a term describing a core level, e.g., a $5p$ level, and its coupling to the $4f$ state

$$H_{5p} = \varepsilon_{5p} \sum_v \psi_{Pv}^\dagger \psi_{Pv} + U_{fc}' \left[N_f - \sum_v \psi_{Pv}^\dagger \psi_{Pv} \right] \sum_{v'} n_{v'} \, , \tag{2.3}$$

where we have assumed also the $5p$ level, with energy ε_{5p}, to have the degeneracy N_f.

To describe the photoemission process we introduce the dipole operator

$$V_p = \sum_v \left[\sum_k \tau_k^{(1)} \psi_{k1v}^\dagger \psi_v + \sum_k \tau_k^{(2)} \psi_{k2v}^\dagger \psi_{pv} + \tau_c \psi_v^\dagger \psi_{dv} \right]$$

$$\equiv V_{d1} + V_{d2} + V_r \, . \tag{2.4}$$

The first term describes the direct emission from the $4f$ level into the continuum states $|k1\rangle$, the second the emission from the $5p$ states, and the third the transitions $4d \rightarrow 4f$. $\tau_k^{(i)}$ and τ_c are dipole matrix elements. Since the $5p$ and $4f$ levels have different symmetries and different energies, we assume that V_p couples these states to different continua. Because of the different symmetry and different energies of the $4f$ and $5p$ states, the transitions from these states are assumed to be two different continua, $|k1\rangle$ and $|k2\rangle$, respectively. The kinetic energy of these states is given by

$$T = \sum_{i=1}^{2} \sum_{k,v} \varepsilon_{ki} \psi_{kiv}^\dagger \psi_{kiv} \, . \tag{2.5}$$

Finally we include the Auger decay terms

$$V_A = v_1 \sum_{k,v,v'} (\psi_{k1v}^\dagger \psi_{dv'}^\dagger \psi_{v'} \psi_v + \text{H.c.})$$

$$+ v_2 \sum_{k,v,v'} (\psi_{k2v}^\dagger \psi_{dv'}^\dagger \psi_{v'} \psi_{pv} + \text{H.c.}) \, , \tag{2.6}$$

where v_1 and v_2 are Auger matrix elements. The first term describes the process $4d^9 4f^{n+1} \rightarrow 4d^{10} 4f^{n-1} \epsilon l$ and the second $4d^9 5p^6 4f^{n+1} \rightarrow 4d^{10} 5p^5 4f^n \epsilon l$. In the Coulomb matrix elements describing these processes, one can expand $|r - r'|^{-1}$ in terms of the type $r_>^{-l-1} r_<^l Y_{lm}(r) Y_{lm}(r')$. For both the transitions considered, the term $l=0$ does not give any contribution. The leading contribution is therefore the $l=1$ term, which leads to operators of the type $\psi_{k1,v+v''}^\dagger \psi_{d,v'-v''}^\dagger \psi_{v'} \psi_v$, with $|v''| \leq 1$. For simplicity we only allow $v''=0$. For the $5p$ transition, one could also consider terms $\psi_{k2v}^\dagger \psi_{dv'}^\dagger \psi_{pv'} \psi_v$. Since, however, the $4f$ orbital has a larger overlap with the $4d$ orbital than the $5p$ orbital, we neglect this term.

III. GENERAL FORMALISM

In this section we develop a formalism for resonance photoemission, generalizing the work of Ref. 20 on Auger electron spectroscopy. We essentially follow the

work in Ref. 18. The Hamiltonian is written as

$$H_T = H_A + T + V_p f(t) \, , \tag{3.1}$$

where

$$H_A = H_0 + H_{4d} + H_{5p} + V_A \equiv H + V_A \tag{3.2}$$

and

$$f(t) = f e^{\eta t} (e^{i\omega t} + e^{-i\omega t}) \, . \tag{3.3}$$

The time dependence of $f(t)$ corresponds to an adiabatic switching on of the external electromagnetic field with the frequency ω. In the absence of the term $V_p f(t)$, the ground state satisfies

$$\psi_{kiv} |E_0(N)\rangle = 0, \quad i = 1,2 \, . \tag{3.4}$$

The effect of $V_p f(t)$ can be treated to lowest order, since the external field is too weak to give rise to nonlinear effects in the situations we are interested in. Using lowest-order time-dependent perturbation theory we obtain the correction to the ground-state wave function

$$|\phi(t)\rangle = f e^{\eta t} \frac{1}{E_0(N) + \omega - H_A - T + i\eta} V_p |E_0(N)\rangle \, , \tag{3.5}$$

where we have only considered processes annihilating a photon $[f \sim \exp(-i\omega t)]$ and where we have suppressed an irrelevant phase factor. The number of electrons emitted to the states $|kiv\rangle$ $(v=1,\ldots,N_f)$ per time unit is then

$$P_{ki}(\omega) = N_f \frac{d}{dt} \langle \phi(t) | \psi_{kiv}^\dagger \psi_{kiv} | \phi(t) \rangle \, , \tag{3.6}$$

where we have used (3.4). We introduce the states

$$|\Phi_{kiv}\rangle \equiv \psi_{kiv} \frac{1}{E_0(N) + \omega - H_A - T + i\eta} V_p |E_0(N)\rangle \tag{3.7}$$

and use the identity

$$\frac{1}{z - H_A - T} = \frac{1}{z - H - T} + \frac{1}{z - H - T} V_A \frac{1}{z - H_A - T} \, . \tag{3.8}$$

Since ψ_{kiv} commutes with H we obtain

$$|\Phi_{kiv}\rangle = \frac{1}{z - H - \varepsilon_{ki}} \psi_{kiv} \left[1 + V_A \frac{1}{z - H_A - T} \right]$$

$$\times V_p |E_0(N)\rangle$$

$$\equiv \frac{1}{z - H - \varepsilon_{ki}} |\phi_{kiv}\rangle$$

$$\equiv \frac{1}{z - H - \varepsilon_{ki}} (|\phi_{kiv}\rangle_d + |\phi_{kiv}\rangle_r) \, , \tag{3.9}$$

where $z = E_0(N) + \omega + i\eta$. With the use of Eq. (3.8) we

have rewritten $|\Phi_{kiv}\rangle$ so that the Auger term V_A enters in two places. First, V_A enters explicitly in the numerator. It describes the Auger processes connecting an intermediate state with a final state containing an electron $|kiv\rangle$. This term is treated exactly. Second, V_A enters in H_A in the denominator. This term leads to a broadening of the core level and contributes to the width of the constant initial-state spectra discussed in Sec. V. This term is treated approximately below [Eqs. (3.11)–(3.17)]. The spectrum is then written as[18,20]

$$P_{ki}(\omega)=N_f f^2 2\eta e^{2\eta t}\langle\Phi_{kiv}|\Phi_{kiv}\rangle$$
$$=N_f 2\pi f^2 e^{2\eta t}\langle\phi_{kiv}|\delta(E_0+\omega-H-\varepsilon_{ki})|\phi_{kiv}\rangle \ .$$

$$(3.10)$$

To calculate $|\phi_{kiv}\rangle_r$ we introduce the projection operator

$$Q=\prod_v \psi_{dv}^\dagger \psi_{dv} \tag{3.11}$$

which projects out states with no $4d$ core hole. Its complement is

$$P=1-Q \ , \tag{3.12}$$

which projects out states with $4d$ core hole(s). In the ground state there is no core hole and no continuum electron [see Eq. (3.4)]. The application of V_P to the ground state leads to a state with either a continuum electron or a $4d$ core hole. This remains true even after repeated application of H_A. Thus $\psi_{kiv}V_A$ gives a nonzero result only if it is applied to a state with a $4d$ hole, and we can insert the operator P to the right of V_A in $|\phi_{kiv}\rangle_r$. In the same way we can insert operators P and Q to the left of $V_P\equiv V_r+V_{d1}+V_{d2}$,

$$|\phi_{kiv}\rangle_r=\psi_{kiv}V_A P\frac{1}{z-H_A-T}$$

$$\times(PV_r+QV_{d1}+QV_{d2})|E_0(N)\rangle \ . \tag{3.13}$$

The technique of Ref. 20 yields

$$g_P(z)\equiv P\frac{1}{z-H_A-T}P=\frac{1}{z-H-\Gamma(z)-T}P \tag{3.14}$$

with

$$\hat{\Gamma}=\sum_{i=1}^{2}\sum_{j=1}^{2}\sum_{k,k'}\sum_{v,v',v_1,v_2} \psi_{iv}^\dagger \psi_{v}^\dagger \psi_{dv'}\psi_{kiv}$$
$$\times\frac{v_i v_j}{z-H-T}\psi_{k'jv_1}^\dagger \psi_{dv_2}^\dagger \psi_{v_2}\psi_{jv_1} \ .$$

$$(3.15)$$

where $\psi_{1v}=\psi_v$ and $\psi_{2v}=\psi_{pv}$. We have now transformed $(z-H_A-T)^{-1}$ in Eq. (3.9) into a form suitable for making approximations. We use the fact that the operator Γ only acts on states with a $4d$ hole, due to the operator P to the right in Eq. (3.14). Due to the structure of H_T and since V_p is treated to lowest order, no state can have

both a $4d$ hole and a continuum electron $|ki\rangle$. Therefore we obtain a contribution only if $k=k'$, $v=v_1$, and $i=j$. If we further assume that the density of states for $|ki\rangle$ is a constant ρ_i and that the band is very broad we find

$$\hat{\Gamma}=-i\sum_{i=1}^{2}\tilde{\Gamma}_i\sum_{v,v',v''}\psi_{iv}^\dagger\psi_{v'}^\dagger\psi_{dv'}\psi_{dv''}^\dagger\psi_{v''}\psi_{iv} \ , \tag{3.16}$$

where

$$\tilde{\Gamma}_i=\pi\rho_i v_i^2 \ . \tag{3.17}$$

The complicated broadening operator Γ in (3.15) now has been simplified to a form where its effect can be expressed in terms of the number of f electrons in the system. This is discussed in Secs. IV and V. We furthermore need

$$P\frac{1}{z-H_A-T}Q=g_p(z)PH_A Q\frac{1}{z-H-T} \ . \tag{3.18}$$

Using arguments similar to those above we obtain

$$PH_A Q\frac{1}{z-H-T}(V_{d1}+V_{d2})|E_0(N)\rangle$$
$$=\left[i\gamma_1\sum_{v,v'}\psi_v^\dagger\psi_{dv}\psi_{v'}^\dagger\psi_{v'}+i\gamma_2\sum_v\psi_v^\dagger\psi_{dv}\right]|E_0(N)\rangle \ ,$$

$$(3.19)$$

where

$$\gamma_1=-\pi\rho_1 v_1\tau_1, \quad \gamma_2=-\pi N_f\rho_2 v_2\tau_2 \tag{3.20}$$

and $\tau_k^{(i)}=\tau_i$ is assumed to be a constant. From Eqs. (3.9), (3.14), (3.16), and (3.19) we obtain

$$|\phi_{kiv}\rangle=\left[\tau_i\psi_{iv}+v_i\sum_{v'}\psi_{dv'}^\dagger\psi_{v'}\psi_{iv}g_p(z)\tilde{V}_r\right]|E_0(N)\rangle \ ,$$

$$(3.21)$$

where ψ_{iv} was defined below Eq. (3.15), $g_P(z)$ in Eq. (3.14),

$$\tilde{V}_r=(\tau_c+i\gamma_1 n_f+i\gamma_2)\sum_v\psi_v^\dagger\psi_{dv} \ , \tag{3.22}$$

and $n_f=\sum_v\psi_v^\dagger\psi_v$. The processes contributing to the different terms in Eqs. (3.21) and (3.22) are shown schematically in Fig. 1. Using Eq. (3.10)

$$P_{ki}(\omega)\sim\langle\phi_{kiv}|\delta(E_0+\omega-H-\varepsilon_k)|\phi_{kiv}\rangle \tag{3.23}$$

together with (3.21) and (3.22) we can now calculate the spectrum using one of the methods developed earlier for nonresonant photoemission.[21–23]

IV. $1/N_f$ TREATMENT

The Anderson model is very hard to solve for the parameter range appropriate for Ce, since U is so large that a Hartree-Fock solution is a bad starting point for a many-body treatment of the problem. Instead we use the idea[31] that $1/N_f$ can be treated as a small parameter, where N_f is the degeneracy of the f level. The treatment below is a generalization of our earlier
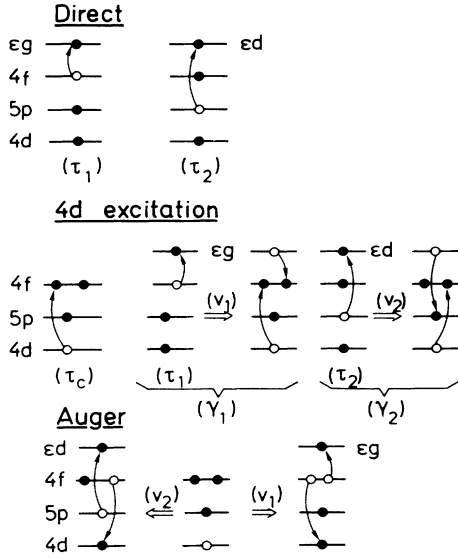
FIG. 1. Schematic representation of the processes contributing to the terms in Eqs. (3.21) and (3.22). The direct processes correspond to the first term in Eq. (3.21) and the combination of a $4d$ excitation and an Auger decay gives a resonance process represented by the second term in (3.21). The different $4d$-excitation processes are described by $\tilde{V}_r$ in Eq. (3.22). The figure on the left shows the $4d \rightarrow 4f$ transition. The following figures illustrate how the same state can be obtained by a $4f \rightarrow \varepsilon g$ transition followed by a $4d\varepsilon g \rightarrow 4f^2$ Auger process, or by a $5p \rightarrow \varepsilon d$ transition followed by a $4d\varepsilon d \rightarrow 5p4f$ Auger process.

work.[21–23,18]

We introduce

$$\tilde{V}(\varepsilon) = \sqrt{N_f}\, V(\varepsilon) \tag{4.1}$$

and require that $\tilde{V}(\varepsilon)$ is independent of N_f.[21] The contribution to the spectra can then be classified in orders of $(1/N_f)$. We consider all terms of order $(1/N_f)^0$ and some terms of order $(1/N_f)^1$. Furthermore we allow for configurations with at most two f electrons in the initial and final states and three f electrons in the intermediate states (with a $4d$ hole).

The ground state is calculated variationally, and we therefore introduce a basis set. The starting point is a Fermi-sea state.

$$| 0 \rangle \tag{4.2}$$

in which all conduction states below the Fermi energy $\varepsilon_F = 0$ are filled and the f level is empty. This couples to the f^1 states

$$| \varepsilon \rangle = \frac{1}{\sqrt{N_f}} \sum_v \psi_v^\dagger \psi_{\varepsilon v} | 0 \rangle \tag{4.3}$$

and the f^2 states

$$| \varepsilon\varepsilon' \rangle = \frac{1}{\sqrt{N_f(N_f-1)}} \sum_{v,v'} \psi_v^\dagger \psi_{\varepsilon v} \psi_{v'}^\dagger \psi_{\varepsilon' v'} | 0 \rangle , \tag{4.4}$$

where $\varepsilon \le \varepsilon_F$, $\varepsilon' \le \varepsilon_F$. In (4.4) $\varepsilon > \varepsilon'$ to avoid a linear dependence. The states (4.2)–(4.4) give the contributions of order $(1/N_f)^0$ to, e.g., the ground-state energy. We also consider the state

$$| E\varepsilon \rangle \frac{1}{\sqrt{N_f}} \sum_v \psi_{Ev}^\dagger \psi_{\varepsilon v} | 0 \rangle , \tag{4.5}$$

which is one of several states of order $(1/N_f)^1$. The ground state is then written as

$$| E_0(N) \rangle = A \left[| 0 \rangle + \int_{-B}^0 d\varepsilon\, a(\varepsilon) | \varepsilon \rangle \right.$$
$$+ \int_{-B}^0 d\varepsilon \int_{-B}^\varepsilon d\varepsilon'\, b(\varepsilon,\varepsilon') | \varepsilon\varepsilon' \rangle$$
$$\left. + \int_0^B dE \int_{-B}^0 d\varepsilon\, c(E,\varepsilon) | E\varepsilon \rangle \right] . \tag{4.6}$$

To perform the calculations we now also introduce basis states for the intermediate states

$$| 1 \rangle = \frac{1}{\sqrt{N_f}} \sum_v \psi_v^\dagger \psi_{dv} | 0 \rangle , \tag{4.7}$$

$$| \varepsilon 1 \rangle = \frac{1}{\sqrt{N_f(N_f-1)}} \sum_{v \ne v'} \psi_v^\dagger \psi_{dv} \psi_{v'}^\dagger \psi_{\varepsilon v'} | 0 \rangle , \tag{4.8}$$

$$| \varepsilon\varepsilon' 1 \rangle = \frac{1}{\sqrt{N_f(N_f-1)(N_f-2)}}$$
$$\times \sum_{v \ne v' \ne v''} \psi_v^\dagger \psi_{dv} \psi_{v'}^\dagger \psi_{\varepsilon v'} \psi_{v''}^\dagger \psi_{\varepsilon' v''} | 0 \rangle , \tag{4.9}$$

$$| E1 \rangle = \frac{1}{\sqrt{N_f}} \sum_v \psi_{Ev}^\dagger \psi_{dv} | 0 \rangle , \tag{4.10}$$

$$| E\varepsilon 1 \rangle = \frac{1}{\sqrt{N_f(N_f-1)}} \sum_{v \ne v'} \psi_v^\dagger \psi_{dv} \psi_{Ev'}^\dagger \psi_{\varepsilon v'} | 0 \rangle , \tag{4.11}$$

$$| E\varepsilon 2 \rangle = \frac{1}{\sqrt{N_f(N_f-1)}} \sum_{v \ne v'} \psi_v^\dagger \psi_{dv} \psi_{Ev'}^\dagger \psi_{\varepsilon v} | 0 \rangle . \tag{4.12}$$

The states (4.7)–(4.9) give contributions of order $(1/N_f)^0$ and the states (4.10)–(4.12) contributions of order $(1/N_f)^1$. These states are consistent with the ground-state basis functions (4.2)–(4.5). A state of the type of (4.11) and (4.12) but with all v indices equal has been neglected, since it does not contribute to order $(1/N_f)^1$. These are the first few states needed in a theory, describing Mahan–Nozières–De Dominici edge singularities. The accuracy was discussed in Ref. 23 for core-level photoemission.

We can now evaluate $\tilde{V}_r | E_0(N) \rangle$ entering in Eq. (3.21),

$$\tilde{V}_r | E_0(N) \rangle = A \left[\tilde{\tau}_c \sqrt{N_f} | 1 \rangle + \int d\varepsilon\, a(\varepsilon)(\tilde{\tau}_c + i\gamma_1)\sqrt{N_f - 1} | \varepsilon 1 \rangle \right.$$
$$\left. + \int d\varepsilon \int d\varepsilon'\, b(\varepsilon,\varepsilon')(\tilde{\tau}_c + 2i\gamma_1)\sqrt{N_f - 2} | \varepsilon\varepsilon' 1 \rangle + \int dE \int d\varepsilon\, c(E,\varepsilon)\tilde{\tau}_c \sqrt{N_f - 1} | E\varepsilon 1 \rangle \right] , \tag{4.13}$$

where $\tilde{\tau}_c = \tau_c + i\gamma_2$. The nonzero matrix elements of the operator Γ are given by

$$\langle 1 \mid \hat{\Gamma} \mid 1 \rangle = -iN_f \Gamma_2 \ , \tag{4.14}$$

$$\langle \varepsilon 1 \mid \hat{\Gamma} \mid \varepsilon'1 \rangle = -i(N_f - 1)(\Gamma_1 + \Gamma_2)\delta(\varepsilon - \varepsilon') \ , \tag{4.15}$$

$$\langle \varepsilon\varepsilon'1 \mid \hat{\Gamma} \mid \varepsilon_1\varepsilon_21 \rangle = -i(N_f - 2)(2\Gamma_1 + \Gamma_2)\delta(\varepsilon - \varepsilon_1)\delta(\varepsilon' - \varepsilon_2) \ , \tag{4.16}$$

$$\langle E\varepsilon 1 \mid \hat{\Gamma} \mid E'\varepsilon'1 \rangle = -i(N_f - 1)\Gamma_2\delta(E - E')\delta(\varepsilon - \varepsilon') \ , \tag{4.17}$$

where $\Gamma_1 = \tilde{\Gamma}_1$ and $\Gamma_2 = N_f\tilde{\Gamma}_2$. All other matrix elements of Γ are zero.

We further have to calculate $g_p(z)$ in Eq. (3.14). This involves the inversion of the matrix $\tilde{H}(\omega) = z - H - \Gamma(z)$, since T gives no contribution for the states of interest. The calculations are simplified and the physics becomes more transparent, if the blocks of $\tilde{H}(z)$ corresponding to the states (4.11) and (4.12) are "folded" (using the Löwdin partitioning technique), followed by a "folding" of the states (4.10). We then have to invert the matrix

$$\tilde{H}_{11}(\omega) = \omega - z_1 - C_M^2 \int \frac{V(E)^2}{K(E)} dE \ , \tag{4.18}$$

$$\tilde{H}_{\varepsilon,\varepsilon'}(\omega) = \left[\omega - z_2 + \varepsilon - C_M^2 \int \frac{V(E)^2 dE}{\omega - z_1' + \varepsilon - E} - C_M^2 \int \frac{V(E)^2 dE}{\omega - \tilde{z}_1 + \varepsilon - E} \right] \delta(\varepsilon - \varepsilon')$$

$$\quad - C_M^4 V(\varepsilon)V(\varepsilon')(N_f - 1) \int \frac{V(E)^2}{K(E)(\omega - \varepsilon - E - \tilde{z}_1)(\omega + \varepsilon' - E - \tilde{z}_1)} \ , \tag{4.19}$$

$$\tilde{H}_{\varepsilon\varepsilon',\varepsilon_1\varepsilon_2}(\omega) = (\omega - z_3 + \varepsilon + \varepsilon')\delta(\varepsilon - \varepsilon_1)\delta(\varepsilon' - \varepsilon_2) \ . \tag{4.20}$$

The nonzero, nondiagonal matrix elements $\tilde{H}_{1,\varepsilon}(\omega)$ and $\tilde{H}_{\varepsilon,\varepsilon'\varepsilon''}(\omega)$ are not shown here. The notations 1, ε, and $\varepsilon\varepsilon'$ refer to the states (4.7), (4.8), and (4.9), respectively. We have used the notations

$$z_1 = \overline{\varepsilon}_f - iN_f\Gamma_2 + \varepsilon_M^{(1)} + z_0 \ , \tag{4.21}$$

$$z_2 = 2\overline{\varepsilon}_f + U - i(N_f - 1)(\Gamma_1 + \Gamma_2) + \varepsilon_M^{(2)} + z_0 \ , \tag{4.22}$$

$$z_3 = 3\overline{\varepsilon}_f + 3U - i(N_f - 2)(2\Gamma_1 + \Gamma_2) + \varepsilon_M^{(3)} + z_0 \ , \tag{4.23}$$

$$K(E) = \omega - z_0 - E - (N_f - 1)C_M^2 \int_{-B}^{0} \frac{V(\varepsilon)^2 d\varepsilon}{\omega - \tilde{z}_1 - E + \varepsilon} \ , \tag{4.24}$$

where $\overline{\varepsilon}_f = \varepsilon_f - U_{fc}$, $z_0 = -\Delta E - \varepsilon_{4d}$, and $\Delta E = E_0(N) - \langle 0 \mid H \mid 0 \rangle$. We have also used the notations $z_1' = z_1 + i\Gamma_2$ and $\tilde{z}_1 = z_1 + i(N_f - 1)\Gamma_2$. For the numerical treatment it is convenient to fold the block (4.20) into the rest of the matrix. The resulting matrix can easily be inverted. Using "backfolding" we obtain the full matrix $g_p(z)$. Combining this with Eq. (4.13), we obtain $g_p\tilde{V}_r \mid E_0(N) \rangle$ needed in (3.21). It is then straightforward to calculate $\mid \phi_{kiv} \rangle$. The $P_{ki}(\omega)$ in (3.10) can then be evaluated using one of the methods developed earlier for nonresonant photoemission.[21-23]

V. RESULTS FOR RESONANCE VALENCE PHOTOEMISSION

We here focus on the constant-initial-state (CIS) spectrum,

$$P_i^{CIS}(\varepsilon,\omega) = \sum_k P_{ki}(\omega)\delta(\varepsilon - \varepsilon_k + \omega) \tag{5.1}$$

which shows how probability for emission from states with binding energy $\mid \varepsilon \mid$ depends on the photon energy ω. This dependence is dominated by the Fano effect.[32] This results from the interference of the two terms in Eq. (3.21) corresponding to a direct process (first term) and a resonance process (second term). The most important contributions to g_P in the second term behave approximately as

$$\frac{1}{\omega - z_2} \ , \tag{5.2}$$

which can be obtained from Eq. (4.19). For simplicity we neglect the terms $[\sim C_M^2 V(E)^2]$ of order $(1/N_f)$. Equation (5.2) is negative for small values of ω and positive for large values of ω. With the sign of τ_1 used in Fig. 2, this leads to destructive (constructive) interference far below (above) the resonance energy $\varepsilon_r = \text{Re}z_2$, if $\gamma_1 = \gamma_2 = 0$ (top curve). This interference displaces the maximum of the curve from $\omega = \varepsilon_r$. In general γ_1 and γ_2 are nonzero. As can be seen from Eqs. (3.13) and (3.18)–(3.22) the corresponding terms in (3.22) result from processes where a $4f$ electron or a $5p$ electron is first emitted. In a following ("reversed") Auger process it falls back into its level and a $4d \rightarrow 4f$ excitation takes place. This is followed by an Auger process and the emission of an electron. Since this chain of processes involves an intermediate state with a $4d$ hole, it contributes to the resonance amplitude. The terms containing γ_1 and γ_2 give, however, a complex phase to the resonance amplitude also far away from $\omega = \varepsilon_r$. For $\gamma_1, \gamma_2 \gg \tau_c$ it is therefore not meaningful to talk about constructive or destructive interference and the photon-energy dependence is strongly modified. This is illustrated in Fig. 2, which shows results to lowest order in $1/N_f$. To keep the relative im-
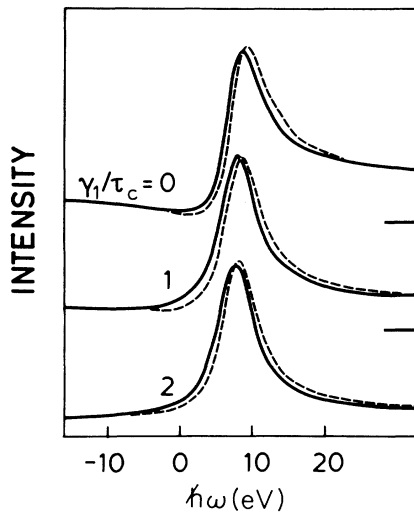
FIG. 2. The CIS spectrum for $\varepsilon = -0.2$ eV (solid line) and $\varepsilon = -2.2$ (dashed line) as a function of τ_c and γ_1 [see Eq. (3.22)]. All curves are renormalized to their maximum value. Here and in the following, the zero of the photon energy ω is arbitrary. The parameters are $\varepsilon_f = -2$ eV, $N_f \Delta = 0.88$ eV, $U = 6$ eV, $U_{fc} = -8$ eV, $B = 6$ eV, $(N_f - 1)\Gamma_1 = 2.75$ eV, $\Gamma_2 = 0$, $\gamma_2 = 0$, $\tau_1 = 0.75$, $\varepsilon_M^{(1)} = 0$, $\varepsilon_M^{(2)} = 20$ eV, and $\varepsilon_M^{(3)} = 18$ eV.

portance of the direct and resonance processes fixed, the value $\tau_c^2 + \gamma_1^2 = 0.29^2$ is kept unchanged. As γ_1 is increased the line shape becomes increasingly symmetric. The parameters are chosen such that the lowest intermediate f^2 and f^3 configurations are degenerate. If there is only one decay process, Γ is not independent of the other parameters. In general, however, there are several decay processes and we have therefore not related Γ to the other parameters. For $V(\varepsilon)$ we use the model

$$\pi V(\varepsilon)^2 = \begin{cases} \Delta[1 - (\varepsilon/B)^2]^{1/2}, & -B \leq \varepsilon \leq 0 \\ \Delta, & 0 \leq \varepsilon \leq B' \\ 0, & \text{otherwise}, \end{cases} \quad (5.3)$$

where B and B' are the bottom and the top, respectively, of the conduction band. This relatively structureless form of $V(\varepsilon)$ is often used for general considerations, since it is not unreasonable and since it does not introduce any peculiar structures in the spectra. In the discussion of specific systems, one should, however, use a more realistic $V(\varepsilon)$.[2,23] In the following we assume that $\gamma_1 = \gamma_2 = 0$, since we have no reliable estimates of these parameters.

In Eq. (5.2) we assumed that the imaginary part of the denominator, which determines the width of the Fano line shape, is just a complex number. As can be seen from Eqs. (4.18)–(4.20) this c-number has to be replaced by an operator, which gives different results depending on the number of f electrons in the state it is applied to. Thus there is an imaginary part due to the Auger process $4d^9 4f^{n+2} \to 4d^{10} 4f^n \varepsilon g$, which is 0, $(N_f - 1)\Gamma_1$, and $(N_f - 2)2\Gamma_1$ for f^1, f^2, and f^3 intermediate states, re-

spectively. This quantity depends strongly on the number of f electrons. In particular it is 0 for f^1 states, since the Auger process under consideration is not possible for these states. The Auger process $4d^9 5p^6 4f^{n+1} \to 4d^{10} 5p^5 4f^n \varepsilon g$ gives the contributions $N_f \Gamma_2$, $(N_f - 1)\Gamma_2$, and $(N_f - 2)\Gamma_2$ for f^1, f^2, and f^3 states, respectively. This process has a weak dependence on the number of f electrons and it is possible also for f^1 states. Finally there is a contribution due to an f electron hopping to a conduction state. This term is proportional to $C_M^2 V(E)^2$ and $2C_M^2 V(E)^2$ for the f^1 and f^2 states, since either of the two f electrons can hop from the f^2 states. There is no such term for the f^3 states in our treatment, since we have not included the corresponding basis states. For the f^3 states the structure would, however, be more complicated, since there would be both a contribution to the diagonal $[\sim 3C_M^2 V(E)^2]$ and to the nondiagonal matrix elements.

In Fig. 3 we illustrate the dependence on Γ_1 (Auger process involving two $4f$ electrons) and Γ_2 (Auger process involving one $4f$ and one $5p$ electron). The calculation is to lowest order in $1/N_f$, and there is, therefore, no broadening due to the hopping of an f electron into the unoccupied conduction states. In the figure we keep the total imaginary part $(N_f - 1)(\Gamma_1 + \Gamma_2)$ [see Eqs. (4.19) and (4.22)] for the (most important) f^2 states fixed. The Fano line shape of the curves is therefore similar in the different cases. Since, however, we vary Γ_1 and Γ_2 individually, the broadening for the f^3 states is different in the three cases studied in Fig. 3. The deviation between the CIS curves for $\varepsilon = -0.2$ and 2.2 eV is therefore different in the three cases. Nevertheless, the $\varepsilon = -0.2$ eV CIS spectrum is found to resonate at a lower energy in all the cases studied, and the qualitative result is therefore rather independent of the relative size of Γ_1 and Γ_2.

In Fig. 4 we finally illustrate the effects of the hopping of f electrons into the unoccupied conduction band. For
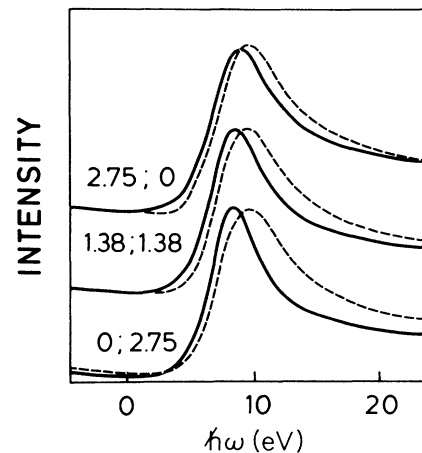
FIG. 3. The CIS spectrum for $\varepsilon = -0.2$ eV (solid line) and $\varepsilon = -2.2$ eV (dashed line) as a function of Γ_1 and Γ_2. The numbers at the curves show the values of $(N_f - 1)\Gamma_1$ and $(N_f - 1)\Gamma_2$, respectively. All curves are renormalized to their maximum values. We have used $\tau_c = 0.29$, $\gamma_1 = \gamma_2 = 0$, and otherwise the same parameters as in Fig. 2.
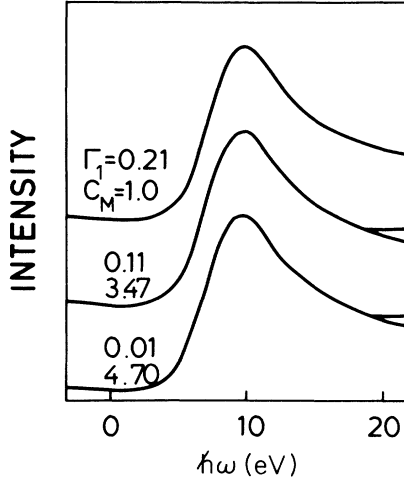
FIG. 4. The CIS spectrum for $\varepsilon = -0.2$ eV as a function of Γ_1 and c_M [see Eq. (2.2)]. The curve for $\varepsilon = -2.2$ eV is identical to within the plotting accuracy. Initial and final f^2 states and intermediate f^3 states are suppressed. We have used the parameters $\tau_c = 0.29$, $\gamma_1 = \gamma_2 = \Gamma_2 = 0$, and otherwise the same parameters as in Fig. 2.

FIG. 5. The CIS spectrum for $\varepsilon = -0.2$ eV (solid line) and $\varepsilon = -2.2$ eV (dashed line) as a function of $\varepsilon_M^{(3)} - \varepsilon_M^{(2)}$. We have used the parameters $\gamma_1 = \gamma_2 = 0$, $\varepsilon_M^{(2)} = 20$ eV, and otherwise the same parameters as in Fig. 2. The values of $\varepsilon_M^{(3)} - \varepsilon_m^{(2)}$ are chosen such that the energy separations of the intermediate f^3 and f^2 states are 3, 0, and -3 eV.

this purpose we have included the state (4.5) in the ground-state calculation and the states (4.10)–(4.12) in the calculation of g_P. Contributions of the order $(1/N_f)^1$ are therefore included. Since we have not included the states of order $(1/N_f)^1$ necessary to give a broadening of the intermediate f^3 states, we suppress these states as well as the initial and final f^2 states. As we illustrate below, the intermediate f^3 states are crucial for the difference between the CIS curves for $\varepsilon = -0.2$ and -2.2 eV. In Fig. 4 these two CIS curves are therefore identical. In the figure we vary Γ_1 (Auger process involving two $4f$ electrons) and C_M (determining the hopping strength in the intermediate state) in such a way that the imaginary part of Eq. (4.19) (the broadening of the f^2 states) stays fixed. The CIS curves are then found to be independent of the mechanism for the broadening. It should, however, be observed that the intermediate f^3 states obtain a different broadening from hopping and Auger decay. If these were included in the theory, we would expect quantitative deviations between the three CIS curves, in analogy with Fig. 3. The situation would, however, be somewhat more complex in this case since the hopping into the unoccupied conduction band could also couple different f^3 states (but not f^2 states) to each other, giving a nondiagonal imaginary part in Eq. (4.20).

As discussed in the Introduction, it has been found experimentally that the maximum in the CIS spectrum is shifted to a lower photon energy for the structure at $\varepsilon = 0$ than for the peak at $\varepsilon = -2$ eV. In Fig. 5 we show calculations of the CIS spectrum to lowest order in $1/N_f$ and neglecting the $5p$ Auger decay. The Fano line shape is then determined by the $4f$ Auger decay. As discussed in the context of Figs. 3 and 4 the neglect of
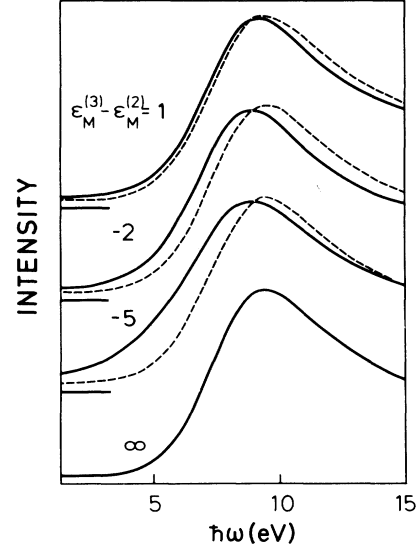
other broadening mechanisms influences the quantitative results. For the qualitative discussion of why the $\varepsilon = 0$ peak resonates at a lower photon energy, the neglected mechanisms are, however, probably not decisive. We have used $\varepsilon_M^{(2)} = 20$ eV and since we have no estimates of $\varepsilon_M^{(3)} - \varepsilon_M^{(2)}$, we have used the values -5, -2, and 1 eV for this quantity. The results depend quantitatively on $\varepsilon_M^{(3)} - \varepsilon_M^{(2)}$, but the maximum of the $\varepsilon = 0$-eV curve is displaced to lower photon energies for all the values considered. The figure also shows results ($\varepsilon_M^{(3)} - \varepsilon_M^{(2)} = \infty$) for the case when the initial and final f^2 configurations and the intermediate f^3 configurations are suppressed. In this case the CIS curves for $\varepsilon = 0$ and -2 eV are practically identical, in disagreement with experiment. This illustrates the importance of including the initial and final f^2 configurations and the intermediate f^3 configurations. The $\varepsilon = -2$ eV peak corresponds to final states of mainly f^0 character, while the $\varepsilon = 0$ eV structure corresponds to final state with a large f^1 character. Thus the intermediate f^2 states couple strongly to the $\varepsilon = -2$ eV peak, since two f electrons are removed in the Auger process. The structure at $\varepsilon = 0$, on the other hand, couples to both the intermediate f^2 and f^3 states. One may then expect the relative energy of the intermediate f^2 and f^3 states to be decisive for which curve resonates at a lower energy. Figure 5 shows that this expectation is incorrect. Below we give a qualitative explanation[18] for the different photon energy dependences.

To simplify the discussion we only consider the resonance term ($\tau_1 = 0$). This changes the line shape and shifts the peak positions, but the difference between $\varepsilon = 0$ and $\varepsilon = -2$ eV remains. Since the $\varepsilon = -2$ eV peak corresponds to final f^0 states it is convenient to introduce

$$f(\omega,\varepsilon)= \sum_i (g_p)_{\varepsilon,i} C_i \ , \tag{5.4}$$

where the index ε of g_p refers to the states (4.8), the index i to any of the states (4.7)–(4.12) and C_i refers to the coefficients in (4.13). For instance, $C_\varepsilon = Aa(\varepsilon)(\tilde{\tau}_c + i\gamma_1)\sqrt{N_f-1}$. The function $f(\omega,\varepsilon)$ describes the coupling to final f^0 states, because two f electrons are removed in the Auger process. Since $a(\varepsilon)$ is large only for ε close to 0, we consider $f(\omega,0)$. The ω

dependence of $f(\omega,0)$ is approximately given by

$$f(\varepsilon,0) \sim \frac{1}{\omega - z_2} \ . \tag{5.5}$$

In the calculation the whole matrix (4.18)–(4.20) must be inverted to obtain q_p and other coefficients C_i must be included. For the parameter range considered, Eq. (5.5) is nevertheless a fair approximation.

The final states contributing to the spectrum close to $\varepsilon = 0$ are[22]

$$|\tilde{\varepsilon}v\rangle = \psi_{\varepsilon v} |E_0(N)\rangle = A \left[|\varepsilon v\rangle + \int_{-B}^0 d\varepsilon' a(\varepsilon') |\varepsilon'\varepsilon v\rangle + \int_{-B}^0 d\varepsilon' \int_{-B}^{\varepsilon'} d\varepsilon'' b(\varepsilon',\varepsilon'') |\varepsilon'\varepsilon''\varepsilon v\rangle \right] , \tag{5.6}$$

where $|E_0(N)\rangle$, $a(\varepsilon)$, and $b(\varepsilon,\varepsilon')$ were defined in Eq. (4.6) and $|\varepsilon v\rangle = \psi_{\varepsilon v} |0\rangle$ is an f^0 final state. The f^1 and f^2 final states $|\varepsilon'\varepsilon v\rangle$ and $|\varepsilon'\varepsilon''v\rangle$ were defined in Ref. 22. The intermediate f^2 states with the amplitudes $f(\omega,\varepsilon)$, couple to the final f^0 states $|\varepsilon v\rangle$ and the intermediate f^3 states $|\varepsilon\varepsilon'1\rangle$ couple to the f^1 states $|\varepsilon'\varepsilon v\rangle$. Using the folding technique we obtain the amplitude

$$\langle \varepsilon\varepsilon'1 | g_p V_r | E_0(N)\rangle = \frac{A\sqrt{N_f-2}\tau_c b(\varepsilon,\varepsilon')}{\omega - z_3 + \varepsilon + \varepsilon'} + \sqrt{N_f-2}\frac{V(\varepsilon)f(\omega,\varepsilon') + V(\varepsilon')f(\omega,\varepsilon)}{\omega - z_3 + \varepsilon + \varepsilon'} \ , \tag{5.7}$$

where z_3 was defined in Eq. (4.23) and we have, for simplicity, set $\gamma_1 = \gamma_2 = 0$. Then the spectral weight at $\varepsilon = 0$ is proportional to

$$
| \langle \varepsilon = 0, v | \phi_{kiv} \rangle |^2
$$

$$
\sim \frac{A^2}{N_f} \left| \sqrt{(N_f-1)N_f} f(0,\omega) \right.
$$

$$
\left. + \left[\frac{N_f-1}{N_f} \right]^{1/2} \int_{-B}^0 d\varepsilon \frac{(N_f-2)a(\varepsilon)[A\tau_c b(\varepsilon,0) + \sqrt{N_f}V(\varepsilon)f(0,\omega) + \sqrt{N_f}V(0)f(\varepsilon,\omega)]}{w - z_3 + \varepsilon} \right|^2 . \tag{5.8}
$$

Combining (5.5) and (5.8) we obtain the semiquantitative approximation

$$
| \langle \varepsilon = 0, v | \phi_{k1v} \rangle |^2 \sim \left| \frac{\alpha}{\omega - z_2} + \frac{\beta}{(\omega - z_2)(\omega - z_3)} + \frac{\kappa}{\omega - z_3} \right|^2 , \tag{5.9}
$$

where α, β, and κ can be estimated from the quantities in (5.8). Similar results are obtained by using the zero-bandwidth limit, discussed in Sec. VI for the core spectrum. The relative signs are such that all three terms interfere constructively for $\omega \ll \mathrm{Re}z_2$ and $\omega \ll \mathrm{Re}z_3$. For the parameters considered here, the first and third terms have approximately the same phases also for larger values of ω. The phase of the second term, however, increases by 2π when ω grows from small values to large values, while the phases of the other two terms only increase by π. The result is a constructive interference for small photon energies and a partly destructive interference for larger photon energies. This displaces the maximum of Eq. (5.9) to lower photon energies than the maximum of Eq. (5.5), at least for the parameters we have considered. This results from the presence of both intermediate f^2 and f^3 states and from the interaction between these.

In Fig. 6 we show spectra for different photon energies. The photon-energy zero is the energy where the Fermi energy structure has its maximum and the curves are normalized to the $\varepsilon = -2$ eV peak. For $\hbar\omega = 15$ eV

and $\hbar\omega = -15$ eV the curves are weakly influenced by the resonance. For $\hbar\omega = -3$ eV, somewhat below resonance, the $\varepsilon = 0$ peak is enhanced, while the other curves show rather small differences.

VI. RESULTS FOR RESONANCE CORE-LEVEL PHOTOEMISSION

The theory developed in Sec. III can also be applied to the emission from core levels. For the Ce $4d$ resonance the core levels of interest are $5s$ and $5p$. Because of the large multiplet coupling in the final states between the $4f$ and $5s$ or $5p$ electrons, the comparison of our theory, which neglects multiplet effects, with experiment is not straightforward. Instead we study UO_2, where the $3d$ resonance photoemission spectrum from the $4f$ core level has been measured.[7] A study of the $4f$ core-level spectrum[33] has provided estimates of the parameters for UO_2. This leads to a picture where the initial state is a linear combination of $5f^2$ and $5f^3$ configurations, with most of the weight in the $5f^2$ configuration. The hybridization Δ is found to be very large ($N_f\Delta \sim 11$ eV),
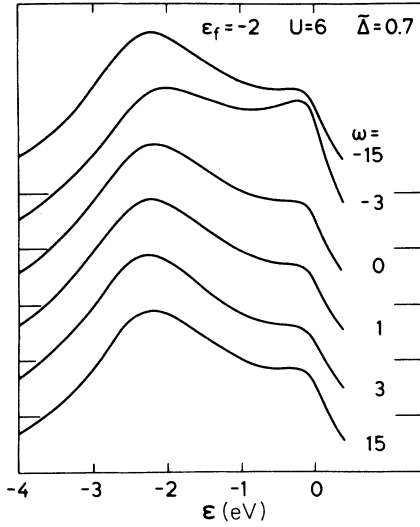
FIG. 6. The spectrum $P_i^{CIS}(\varepsilon,\omega)$ for different values of ω. The maximum of $P_i^{CIS}(-0.2,\omega)$ as a function of ω defines the zero of ω. The parameters are $\varepsilon_f = -2$ eV, $U = 6$ eV, $N_f \Delta = 0.7$ eV, and $B = 6$ eV. A Lorentzian broadening of 0.6 eV (FWHM) was introduced. The intermediate f^2 and f^3 configurations are degenerate.

and in the presence of a core hole the $5f^3$ configuration is only slightly higher than the $5f^2$ configuration. The $4f$ core spectrum has a satellite at about 7 eV higher binding energy than the main peak. Because of the large hybridization these peaks cannot be assigned to final states consisting of mainly one configuration. Instead we find that the main peak (the satellite) corresponds to a bonding (antibonding) linear combination of the $5f^2$ and $5f^3$ configurations, with a comparable weight of both configurations.[33] The basic resonance process in this case is

$$3d^{10}4f^{14}5f^2 \rightarrow 3d^9 4f^{14}5f^3 \rightarrow 3d^{10}4f^{13}5f^2 \epsilon g \ . \quad (6.1)$$

Since both the main line and the satellite correspond to final states containing comparable amount of $5f^2$ character, one may expect both to have similar CIS spectra, in contrast to the experimental results.[7]

To test these arguments we have performed calculations[33] for UO_2. For this purpose we map the U problem on the Ce problem. The energy of the f-electron system is

$$E(n_f) = n_f \varepsilon_f + \tfrac{1}{2}U n_f(n_f - 1) \ , \quad (6.2)$$

where n_f is the number of f electrons. We introduce $\Delta n_f = n_f - n$ and obtain

$$E(n_f) = \Delta n_f \tilde{\varepsilon}_f + \tfrac{1}{2}U \, \Delta n_f(\Delta n_f - 1) + E_0(n) \ , \quad (6.3)$$

where $\tilde{\varepsilon}_f = \varepsilon_f + Un$ and $E_0(n)$ is independent of Δn_f. For UO_2 we are interested in the $5f^2$, $5f^3$, and $5f^4$ configurations. By putting $n = 2$ we map the problem onto Ce, since we then consider $\Delta n_f = 0$, 1, and 2. This approach neglects that the matrix elements connecting

different configurations have n-dependent prefactors. This approach also neglects multiplet effects, which may be important for U compounds in general, but are probably less important for UO_2 because of the strong hybridization.

In the choice of model for the decay process in Sec. II we neglected terms of the type $\psi_{k2v}^\dagger \psi_{dv'}^\dagger \psi_{pv'} \psi_v$, where pv' now would stand for a $4f$ level. For UO_2 these terms would be strongly favored by the matrix elements, because of the $4f$ wave function has a larger overlap with the $3d$ wave function than the $5f$ wave function. Developing a theory including these decay terms instead of the ones included in Sec. II, we obtain a theory with a similar structure as above. We find, however, that in (3.19) the contribution $(\sim \gamma_2)$ from the $4f$ core decay term is reduced by a factor $\sim N_f$. In a similar way the corresponding contribution $(\sim \Gamma_2)$ to Γ is reduced by a factor $\sim N_f^2$. This makes it less obvious which terms should be included to describe the decay involving a $4f$ electron. At the present level of sophistication, where the parameters (e.g., Γ_1 and Γ_2) describing the decay are treated as adjustable, the choice of the model for decay appears less crucial, in particular since the discussion below only uses the fact that the decay gives a broadening. For simplicity, we therefore use the model discussed in Sec. II also for UO_2. At the bottom of Fig. 7 we show the CIS spectra for the main peak and the satellite. The results are in fair agreement with experiment.[7,34] The figure illustrates that contrary to the simple arguments presented above, the two CIS curves are quite different. We find that as in the case of the $4f$ valence spectrum for Ce, interference effects play a very important role also here.

To discuss these results we consider a simple model where the conduction-bandwidth is assumed to be zero. We further neglect the initial $5f^4$ configurations. We are then left with a two-level model, where the two levels $|1\rangle$ and $|2\rangle$ correspond to the initial $5f^2$ and $5f^3$ configurations. These levels are assumed to couple with a strength $-\tilde{V}$. The ground state can then be written as

$$|E_0(N)\rangle = a_1 |1\rangle + a_2 |2\rangle \ , \quad (6.4)$$

where a_1 and a_2 are appropriate coefficients. In the presence of a core hole (intermediate states) we consider states of the type $\psi_v^\dagger \psi_{dv} |i\rangle$, where $i = 1$ or 2. The function g_p can now easily be calculated [see Eqs. (4.18) and (4.19)] and we find

$$(g_p)_{11} = [\omega - z_1 - \tilde{V}^2/(\omega - z_2)]^{-1} \ , \quad (6.5)$$

$$(g_p)_{12} = (g_p)_{21} = (g_p)_{11} \tilde{V}/(\omega - z_2) \ , \quad (6.6)$$

$$(g_p)_{22} = [\omega - z_2 - \tilde{V}^2/(\omega - z_1)]^{-1} \ . \quad (6.7)$$

Finally the appropriate final states, in the presence of a $3d$ core hole, can be written as

$$|E_0(N-1)\rangle = C_1 |1\rangle + C_2 |2\rangle \ , \quad (6.8)$$

$$|E_1(N-1)\rangle = C_2 |1\rangle - C_1 |2\rangle \ . \quad (6.9)$$

Combining Eqs. (3.10), (3.21), (4.13), (6.8) and (6.9) we obtain the weights for the main peak (I_0) and the satellite (I_1) as

$$I_0(\omega) \sim \left| \tau_2(a_1c_1 + a_2c_2) + \tau_c v_2\{N_f a_1 c_1(g_p)_{11} + \sqrt{N_f(N_f-1)}[c_2 a_1(g_p)_{21} + c_1 a_2(g_p)_{12}] + (N_f-1)c_2 a_2(g_p)_{22}\} \right|^2 ,$$

$$(6.10)$$

$$I_1(\omega) \sim \left| \tau_2(a_1c_2 - a_2c_1) + \tau_c v_2\{N_f c_2 a_1(g_p)_{11} + \sqrt{N_f(N_f-1)}[c_2 a_2(g_p)_{12} - c_1 a_1(g_p)_{21}] - c_1 a_2(N_f-1)(g_p)_{22}\} \right|^2 .$$

$$(6.11)$$

The term proportional to τ_2 is the direct term and the one proportional to τ_c is the resonance term. These formulas provide a semiquantitative description of the CIS spectra, if intermediate $5f^5$ configurations are neglected. To understand these results, we first assume that the ground state has only $5f^2$ character $(a_1 = 1, a_2 = 0)$. From Eqs. (6.6), (6.10) and (6.11) we obtain

$$I_0(\omega) = |c_1|^2 \left| \tau_2 + \tau_c v_2 N_f \left[1 + \left(\frac{N_f-1}{N_f} \right)^{1/2} \frac{c_2 \tilde{V}/c_1}{\omega - z_2} \right] (g_p)_{11} \right|^2 ,$$

$$(6.12)$$

$$I_1(\omega) = |c_2|^2 \left| \tau_2 + \tau_c v_2 N_f \left[1 - \left(\frac{N_f-1}{N_f} \right)^{1/2} \frac{c_1 \tilde{V}/c_2}{\omega - z_2} \right] (g_p)_{11} \right|^2 .$$

$$(6.13)$$

These equations can be understood as follows. The $3d \rightarrow 5f$ excitation creates an intermediate $5f^3$ configuration. The amplitude is proportional to $(g_p)_{11}$ and it contributes the second term $\tau_c v_2 N_f(g_p)_{11}$ in (6.12) and (6.13). If this was the only contribution (vanishing third term) the two CIS spectra would have identical

FIG. 7. The CIS spectrum for the UO_2 $4f$ core spectrum. The bottom curve shows the full calculation. For the middle curve initial $5f^4$, intermediate $5f^5$, and final $5f^4$ configurations were suppressed. For the top curve the initial $5f^3$ configurations were in addition suppressed. We have used the parameters $\varepsilon_f = 7.1$, $U = 4$, $\Delta_{av} = 0.76$, $U_{fc} = 6.7$, $\tau_2 = 1.2$, $\tau_c v_2 = 0.25$, $\Gamma_1 = 0$, $\Gamma_2 = 0.18$, $\gamma_1 = 0$, and $\gamma_2 v_2 = 0.18$. All energies are in eV. The valence band was assumed to have a triangular shape extending between 0 and -4 eV, with its maximum at -1 eV. The curves are normalized so that they are identical far from the resonance.

photon-energy dependence and only differ in terms of the absolute intensity. Due to the strong hybridization there is, however, also an intermediate $5f^4$ configuration. In (6.10) and (6.11) its amplitude is given by $(g_p)_{21}$ and in (6.12) and (6.13) by the term proportional to $\tilde{V}$. For $\omega - \text{Re} z_2 \ll \text{Im} z_2$ the $5f^3$ and $5f^4$ configurations have the same phase, and for $\omega - \text{Re} z_2 \gg \text{Im} z_2$ they have the opposite phase. We can also understand this by thinking of the system as being excited into primarily a bonding or an antibonding state, depending on the photon energy. Since the leading peak corresponds to a final bonding combination, it is further enhanced at resonance when the intermediate $5f^4$ configuration is taken into account but less enhanced for $\omega - \text{Re} z_2 \gg \text{Im} z_2$. For the satellite, which corresponds to an antibonding final state, the effect is the opposite. This is illustrated at the top of Fig. 7. In this case the parameters are such that the prefactor of $(g_p)_{11}$ in (6.13) is slightly negative close to resonance and the satellite is somewhat suppressed. In the middle part of Fig. 7 we have included the initial $5f^3$ configurations. There is now a direct transition to intermediate $5f^4$ configurations via $(g_p)_{22}$. At resonance this term adds intensity to the satellite and at higher energies it subtracts intensity. To a certain extent the effects of $(g_p)_{21}$ discussed above are therefore cancelled.

Comparison between the middle curve and the bottom curve shows that the inclusion of intermediate $5f^5$ configurations (bottom curve) leads to additional structure. The reason is that the three intermediate configurations can now form three different intermediate states, and the satellite shows a structure at each one.

VII. SUMMARY

Using the quadratic response formalism we have developed a theory for resonance photoemission. This formalism was applied to the Anderson model using the $1/N_f$ expansion. Both the emission from the localized level (f level) and a core level is studied. The photon-energy dependence is strongly influenced by the operator Γ [Eq. (3.16)], which has a strong state dependence [see

Eqs. (4.14)–(4.17)]. We have considered the contributions to this operator due to the Auger decay of two $4f$ electrons as well as the decay of one $4f$ electron and one core electron. We have further considered the broadening due to the tunneling of an f electron into the conduction band [$\sim V(E)^2$ in Eqs. (4.18)–(4.20)]. These different broadening mechanisms lead to quantitative differences (see Fig. 3), although in the case of the tunneling mechanism, where we consider only two configurations, our calculation does not illustrate this effect. Nevertheless, the results are qualitatively similar for the different mechanisms, so that we can discuss some experimental results qualitatively, without any precise knowledge of the relative importance of the different mechanisms. We have studied the $4f$ valence spectrum

of Ce and the $4f$ core spectrum of UO_2. In both cases the spectra have two structures (neglecting the $4f$ spin-orbit splitting) which have different CIS curves. In both cases we provide similar explanations, based on the interference between different intermediate states. We find that it is crucial to consider the $4f^2$ and $4f^3$ configurations for Ce and the $4f^3$, $4f^4$, and (to a lesser extent) the $4f^5$ configurations of UO_2. We expect similar effects to be important also for other applications.

ACKNOWLEDGMENTS

[1] See, e.g., D. W. Lynch and J. Weaver, in *Handbook on the Physics and Chemistry of Rare Earths*, edited by K. A. Gschneider, LeRoy Eyring, and S. Hüfner (North-Holland, Amsterdam, 1987), Vol. 10.

[2] See, e.g., J. W. Allen, S.-J. Oh, O. Gunnarsson, K. Schönhammer, M. B. Maple, M. S. Torikachvili, and I. Lindau, Adv. Phys. **35**, 275 (1986).

[3] R. D. Parks, N. Mårtensson, and B. Reihl, in *Valence Instabilities*, edited by P. Wachter and H. Boppart (North-Holland, Amsterdam, 1982), p. 239.

[4] F. Patthey, B. Delley, W.-D. Schneider, and Y. Baer, Phys. Rev. Lett. **55**, 1518 (1985).

[5] L. I. Johansson, J. W. Allen, T. Gustafsson, I. Lindau, and S. B. Hagström, Solid State Commun. **28**, 53 (1978); W. Lenth, F. Lutz, J. Barth, G. Kalkoffen, and C. Kunz, Phys. Rev. Lett. **41**, 1185 (1978).

[6] This resonance has also been observed for other rare earths. J. W. Allen, L. I. Johansson, R. S. Bauer, I. Lindau, and S. B. M. Hagström, Phys. Rev. Lett. **41**, 1499 (1978); W. Gudat, S. F. Alvarado, and M. Campagna, Solid State Commun. **28**, 943 (1978).

[7] L. E. Cox, W. P. Ellis, R. D. Cowan, J. W. Allen, and S.-J. Oh, Phys. Rev. B **31**, 2467 (1985).

[8] B. Reihl, N. Mårtensson, D. E. Eastman, A. J. Arko, and O. Vogt, Phys. Rev. B **26**, 1842 (1982); A. J. Arko, D. D. Koelling, A. M. Boring, W. P. Ellis, and L. E. Cox, J. Less-Common Met. **722**, 95 (1986).

[9] See, e.g., N. Mårtensson, B. Reihl, and R. D. Parks, Solid State Commun. **41**, 573 (1982).

[10] J. M. Lawrence, J. W. Allen, S.-J. Oh, and I. Lindau, Phys. Rev. B **26**, 2362 (1982).

[11] J. W. Allen, S.-J. Oh, M. B. Maple, and M. S. Torikachvili, Phys. Rev. B **28**, 5347 (1983).

[12] C. Guillot, Y. Ballu, J. Paigne, J. Lecante, K. P. Jain, P. Thiry, R. Pinchaux, Y. Petroff, and L. M. Falicov, Phys. Rev. Lett. **39**, 1632 (1977).

[13] D. R. Penn, Phys. Rev. Lett. **42**, 921 (1979); L. C. Davis and L. A. Feldkamp, *ibid.* **43**, 151 (1979); **44**, 673 (1980); Phys. Rev. B **23**, 6239 (1981); L. C. Davis, *ibid.* **25**, 2912 (1982).

[14] Y. Yafet, Phys. Rev. B **21**, 5023 (1980); **23**, 3558 (1981); S. M. Girvin and D. R. Penn, *ibid.* **22**, 4081 (1980); S.-J. Oh and S. Doniach, Phys. Lett. **81A**, 483 (1981); Phys. Rev. B **26**, 1859 (1982); G. v. d. Laan, Solid State Commun. **42**, 165 (1982). J. C. Parlebas, A. Kotani, and J. Kanamori, J. Phys. Soc. Jpn.

51, 124 (1982); Solid State Commun. **41**, 439 (1982); T. Jo, A. Kotani, J. C. Parlebas, and J. Kanamori, J. Phys. Soc. Jpn. **52**, 2581 (1983).

[15] A. Zangwill and P. Soven, Phys. Rev. Lett. **45**, 204 (1980).

[16] A. Sakuma, Y. Kuramoto, T. Watanabe, and C. Horie, J. Magn. Magn. Mater. **52**, 393 (1985).

[17] P. W. Anderson, Phys. Rev. **124**, 41 (1961).

[18] O. Gunnarsson and K. Schönhammer, in *Giant Resonances in Atoms, Molecules and Solids*, edited by J. P. Connerade, J.-M. Esteva, and R. C. Karnatak (Plenum, New York, 1987), p. 405.

[19] L. Hedin and S. Lundqvist, in *Solid State Physics*, edited by H. Ehrenreich, D. Turnbull, and F. Seitz (Academic, New York, 1969), Vol. 23, p. 1.

[20] O. Gunnarsson and K. Schönhammer, Phys. Rev. B **22**, 3710 (1980).

[21] O. Gunnarsson and K. Schönhammer, Phys. Rev. B **28**, 4315 (1983).

[22] O. Gunnarsson and K. Schönhammer, Phys. Rev. B **31**, 4815 (1985).

[23] O. Gunnarsson and K. Schönhammer, in *Handbook on the Physics and Chemistry of Rare Earths*, edited by K. Gschneider, LeRoy Eyring, and S. Hüfner (North-Holland, Amsterdam, 1987), Vol. 10.

[24] E. Wuilloud, B. Delley, W.-D. Schneider, and Y. Baer, Phys. Rev. Lett. **53**, 202 (1984).

[25] B. Delley and H. Beck, J. Magn. Magn. Mater. **47&48**, 269 (1985).

[26] O. Sakai, H. Takahashi, M. Takeshige, and T. Kasuya, Solid State Commun. **52**, 997 (1984).

[27] N. E. Bickers, D. L. Cox, and J. W. Wilkins, Phys. Rev. Lett. **54**, 230 (1985).

[28] J. F. Herbst, R. E. Watson, and J. W. Wilkins, Phys. Rev. B **17**, 3089 (1978).

[29] A. Kotani and Y. Toyozawa, J. Phys. Soc. Jpn. **37**, 563 (1974); **37**, 912 (1974).

[30] J. Sugar, Phys. Rev. B **5**, 1785 (1972).

[31] P. W. Anderson, in *Valence Fluctuations in Solids*, edited by L. M. Falicov, W. Hanke, and M. P. Maple (North-Holland, Amsterdam, 1981), p. 451; T. V. Ramakrishnan, *ibid.*, p. 13.

[32] U. Fano, Phys. Rev. **124**, 1866 (1961).

[33] O. Gunnarsson, D. D. Sarma, F. U. Hillebrecht, and K. Schönhammer J. Appl. Phys. (to be published).

[34] J. W. Allen (private communication).